*Am J Physiol Cell Physiol* 302: C1004–C1011, 2012.
First published February 1, 2012; doi:10.1152/ajpcell.00422.2011.

# Detailed examination of $Mg^{2+}$ and pH sensitivity of human TRPM7 channels

**Rikki Chokshi,[1] Masayuki Matsushita,[2] and J. Ashot Kozak[1]**

[1]*Department of Neuroscience, Cell Biology, and Physiology, Wright State University, Dayton, Ohio; and* [2]*Department of Molecular and Cellular Physiology, University of the Ryukyus, Okinawa, Japan*

Submitted 30 November 2011; accepted in final form 25 January 2012

**Chokshi R, Matsushita M, Kozak JA.** Detailed examination of $Mg^{2+}$ and pH sensitivity of human TRPM7 channels. *Am J Physiol Cell Physiol* 302: C1004–C1011, 2012. First published February 1, 2012; doi:10.1152/ajpcell.00422.2011.—TRPM7 channel kinase is a protein highly expressed in cells of hematopoietic lineage, such as lymphocytes. Studies performed in native and heterologous expression systems have shown that TRPM7 forms nonselective cation channels functional in the plasma membrane and activated on depletion of cellular $Mg^{2+}$. In addition to internal $Mg^{2+}$, cytosolic pH and the phospholipid phosphatidylinositol-(4,5)-bisphosphate [PI(4,5)$P_2$] are potent physiological regulators of this channel: protons inhibit, while PI(4,5)$P_2$ is required for TRPM7 channel activity. These channels are also inhibited from inside by other metal cations and polyamines. While the regulation of TRPM7 channels by internal metal ions, acidic pH, and PI(4,5)$P_2$ is voltage independent, extracellular metal cations and polyamines block voltage dependently at micromolar concentrations and appear to occupy a distinct blocking site. In the present study we investigated intracellular $Mg^{2+}$ and pH dependence of native TRPM7 currents using whole cell patch-clamp electrophysiology in human Jurkat T lymphocytes and HEK293 cells. Our main findings are *1*) $Mg^{2+}$ inhibition involves not one but two separate sites of high (~10 μM) and low (~165 μM) affinity; and *2*) while sharing certain characteristics with $Mg^{2+}$ inhibition, protons most likely inhibit through one inhibitory site, corresponding to the low-affinity $Mg^{2+}$ site, with an estimated $IC_{50}$ of pH 6.3. Additionally, we present data on amplitude distribution of preactivated TRPM7 currents in Jurkat T lymphocytes in the absence of prior $Mg^{2+}$ or proton depletion.

cation channel; MIC channel; patch clamp; leukocyte; HEK293

THE ORIGINAL MEMBERS of the transient receptor potential (TRP) family of ion channels were discovered in *Drosophila* photoreceptors and represent the light-sensitive $Ca^{2+}$ influx pathway (14, 42). In mammals, the TRP family has 28 members distributed among six subfamilies, one of which is TRPM, named after melastatin (7, 13, 37). TRPM7 channel activity was first identified when the removal of cytoplasmic $Mg^{2+}$ with the aid of a metal chelator revealed a steeply outwardly rectifying current, which was named MIC ($Mg^{2+}$-inhibited cation) (21, 43) or MagNuM ($Mg^{2+}$ nucleotide-regulated metal) (15). These channels have since been described in many mammalian cell types (e.g., 12, 16, 17). TRPM7 is highly expressed in cells of hematopoietic origin, such as leukocytes. It is also expressed in diverse cell lines commonly used by biologists: HEK293, HeLa, CHO-K1, COS-7, RBL, and smooth muscle cells (20, 38, 40). Thus, in channel overexpression studies, one has to be careful and consider that TRPM7 currents are always contaminated with their endogenous counterparts. One approach to this problem is to aim for high levels of recombinant channel expression to increase signal-to-noise ratios of the measurements (see 34).

TRPM7 is one of very few "chanzymes" encoded in the human genome, being composed of a "channel" domain and an "enzyme" domain (1, 36). For this protein, originally named ChaK1 for channel-kinase 1, the enzyme is a functional serine/threonine kinase belonging to the class of atypical kinases that has been crystallized in isolation (32, 56).

TRPM7 is proposed to serve as a key molecule governing cellular $Mg^{2+}$ homeostasis in mammals since its channel pore is permeable to $Mg^{2+}$ ions and can act as a $Mg^{2+}$ influx pathway. It is not selective for $Mg^{2+}$, however, and conducts other divalent metal cations (35, 48, 55).

Interestingly, both channel and kinase activities are dependent on divalent metal ion concentrations. TRPM7 currents are inhibited by internal millimolar free $Mg^{2+}$ and other metal ions such as $Ca^{2+}$, $Zn^{2+}$, $Ba^{2+}$, etc., ions that are permeant through this channel (20, 35). TRPM7 phosphotransferase function is also sensitive to these metals but with a diverging profile: kinase activity is enhanced by $Mg^{2+}$, inhibited by $Zn^{2+}$, but unaffected by $Ca^{2+}$. TRPM7 kinase activity is diminished at both acidic and basic pH, in contrast to channel activity, which is enhanced at basic pH (22). On the basis of these findings and site-directed mutagenesis of the kinase domain, we suggested that the channel and phosphotransferase activities of this protein are separate from each other (34).

While it has been known for a decade that TRPM7 channels are inhibited by $Mg^{2+}$, previous studies reported monotonic reductions of current with increasing intracellular $Mg^{2+}$ concentration ($[Mg^{2+}]_i$), corresponding to dose-response curves with a single ~0.6 mM $IC_{50}$ site (e.g., Refs. 38, 40, 43 for native and overexpressed channels).

We attempted to generate a $Mg^{2+}$ concentration-effect relation for the human TRPM7 native to Jurkat T cells. To this end we introduced *N*-(2-hydroxyethyl)ethylenediaminetriacetic acid (HEDTA) as the metal chelator of choice allowing us to study the widest range of $Mg^{2+}$ concentrations, from nanomolar to hundreds of micromolar. Here we report that TRPM7 channel activity, as measured in whole cell patch clamp, displays a biphasic dose-response curve with high (~10 micromolar)- and low (~165 micromolar)-affinity $Mg^{2+}$ inhibitor sites.

In our earlier study we demonstrated that both native and overexpressed TRPM7 channel activity are sensitive to intracellular pH (22). We did not present a dose-response curve, however. In the present study, to characterize this pH dependence in detail, we have constructed a dose-response relation for the native TRPM7 current of HEK293 cells and found that pH dependence is also biphasic, as with $Mg^{2+}$, if the intracellular solution contains a relatively weak $Mg^{2+}$ chelator. The dose-response relation becomes monotonic when the contaminating micromolar $Mg^{2+}$ is removed by including HEDTA, a

Address for reprint requests and other correspondence: A. Kozak, Biological Sciences Bldg. II, Rm. 148, Wright State Univ., 3640 Colonel Glenn Hwy., Dayton, OH 45435 (e-mail: juliusz.kozak@wright.edu).

strong $Mg^{2+}$ chelator, thus suggesting that protons cannot substitute for $Mg^{2+}$ in all instances of inhibition.

Through construction of a histogram of preactivated TRPM7 currents in Jurkat T cells, we find that a significant fraction of cells displays measurable TRPM7 currents even before $Mg^{2+}$ or pH in the cell are experimentally perturbed. This suggests that TRPM7 channels can function in Jurkat T cells under physiological conditions.

A preliminary report of this study has appeared in abstract form (6).

## MATERIALS AND METHODS

*Cell lines.* The present study was performed using two human cell lines: Jurkat leukemic T lymphocytes and human embryonic kidney (HEK) 293 cells. Jurkat T and HEK293 cells were grown in RPMI-1640 (Lonza, Wakersville, MD) supplemented with 10% fetal bovine serum (BioWest, Nuaille, France). Cells were maintained in a cell culture incubator (Napco 8000) at 37°C under a 95% air-5% $CO_2$ atmosphere. Jurkat T cells were passaged twice a week by 10- to 20-fold dilution in fresh culture medium. HEK293 cells were treated with trypsin-EDTA (Lonza) and seeded at ~1/10 of initial density once a week. Tests to rule out the presence of mycoplasmal contamination were not performed.

*RT-PCR.* Both TRPM7 and TRPM6 and channels have been reported to give rise to $Mg^{2+}$-sensitive cation channels (reviewed in 44). To compare TRPM7 and TRPM6 gene expression in Jurkat T and HEK293 cells, we isolated total RNA from both cell lines and performed reverse transcription-PCR (RT-PCR) experiments with primer sets specific for human TRPM7, TRPM6, and glyceraldehyde-3-phosphate dehydrogenase (GAPDH), a housekeeping gene. Target DNA specificity of the primer sets was evaluated with NCBI Primer-BLAST. Total RNA was isolated by the single-step method using TRI Reagent (Sigma-Aldrich, St. Louis, MO). The purified RNA was treated with DNase I to eliminate possible genomic DNA contamination and quantitated with NanoDrop spectrophotometer (Agilent Technologies). PCR was performed in a programmable thermal cycler (Applied Biosystems). The sequences of human TRPM7 (hTRPM7)-specific primers were 5′-CTGAAGAGGAATGATTATACGCC-3′ and 5′-GCCTAACCCTGATTCATAAA-3′. The hTRPM6-specific primers had the sequences 5′-AAGTATATGACAGGGGAGTT-3′ and 5′-CAGGAGTTACAATGATGTTT-3′. PCR reaction products were visualized by 0.8% agarose gel electrophoresis. Equal amounts of reactions were loaded in all wells as confirmed by similar intensity of GAPDH bands. In both cell lines strong TRPM7 expression was detected but no TRPM6-specific signal found (Fig. 1), thus confirming that all the electrophysiological recordings reported in this study likely represent the activity of the native TRPM7 channels and not TRPM6 channels.

*Patch-clamp electrophysiology.* Native TRPM7 currents were recorded as previously described (21). The standard intracellular solution contained HEDTA (Acros Organics, Geel, Belgium) as the metal ion chelator; its complete composition was 130 mM Cs glutamate, 8 mM NaCl, 0.09 $CaCl_2$, 10 mM HEDTA, 5 mM CsF, 10 mM HEPES, pH 7.3. $MgCl_2$ was added to this solution to achieve the free $Mg^{2+}$ concentrations ($[Mg^{2+}]$) necessary to construct a dose-response curve. Free $[Mg^{2+}]$ was estimated by MaxChelator software available at http://www.stanford.edu/~cpatton/webmaxcS.htm. Throughout the article we refer to current magnitude reduction by $Mg^{2+}$ as "inhibition" to distinguish it from a pore block mechanism (18, 23). Internal $Cs^+$ was used to block $K^+$ channels (10, 58). Inclusion of HEDTA and low $Ca^{2+}$ concentration ($[Ca^{2+}]$) prevented activation of the $Ca^{2+}$-activated TRPM4 channels reported to be expressed Jurkat T lymphocytes (25). The normal bath (extracellular) solution contained 2 mM $CaCl_2$, 4.5 mM KCl, 140 mM Na aspartate, 10 mM HEPES-$Na^+$, pH 7.3. Pipettes were manufactured from borosilicate capillary glass (Warner Instrument, Hamden, CT) on a robotic puller (Zeitz Instruments, Martinsried, Germany) and had resistances of 1.4–3.5 mΩ when filled with the internal solutions. Recordings were made with EPC10 (HEKA Elektronik, Germany) computer-driven patch-clamp amplifier operated by Patchmaster software (v. 2.6). Command voltage ramps of 211-ms duration ranging from −100 to +85 mV were applied every 2.5 s and the resultant instantaneous current-voltage relations stored for further analysis. The cell was held at 0 mV between the ramps. Current signals were filtered at 2.9 kHz and digitized at 5 kHz. Current traces and time courses were exported to Origin v.8 software (OriginLab, Northampton, MA) for further analysis and graphing. Origin was also used to fit dose-response curves depicted in Figs. 2–4 and histograms depicted in Fig. 5.

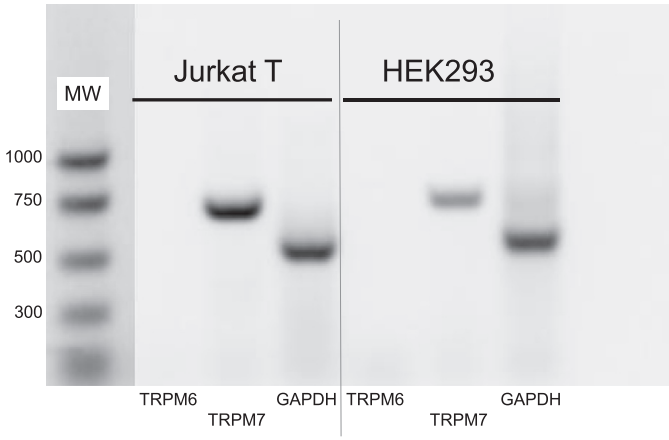


Fig. 1. RT-PCR with with Jurkat and HEK293 cell total RNA. RNA isolated from Jurkat T lymphocytes grown in suspension (*left*) and HEK293 cells grown in a monolayer (*right*) were used for RT-PCR reactions with melastatin-like transient receptor potential (TRPM) 6-, TRPM7-, and GAPDH-specific primer sets (40 cycles). Predicted sizes of the respective products are 284, 734, and 555 bp (NCBI Primer-BLAST). Amplified fragments were separated by electrophoresis in a 0.8% agarose gel with added ethidium bromide. *Left lane*: DNA molecular weight (MW) marker (Hi-Lo DNA marker, Minnesota Molecular). All 6 reactions were electrophoresed on the same gel; the vertical line is added for visual aid. The contrast of MW lane was enhanced separately to improve resolution.

Experiments done to determine the pH sensitivity of TRPM7 channels were performed with the standard internal solution (see above) and with an internal solution containing 12 mM EGTA (used previously in Refs. 21, 22) instead of 10 mM HEDTA. The pH was adjusted on the day of experiment. At intracellular pH ($pH_i$) values of 6.5 and lower, a cation current was activated in HEK293 cells (~300–400 pA/cell) that tended to run down after several minutes of whole cell perfusion. TRPM7 current magnitude in these cases was measured after the proton-activated current ran down completely (discussed in Ref. 22). Recordings in which the proton-activated current became persistent were not used in this study.

*Preactivation measurements.* Data for preactivated TRPM7 current amplitude histograms (Fig. 5) were obtained from recordings with $Mg^{2+}$-free (12 EGTA or 10 HEDTA) and 16, 40, and 60 μM $MgCl_2$-containing solutions, corresponding to calculated free $Mg^{2+}$ concentrations of 106, 266, and 399.5 nM. Only recordings with low pipette $Mg^{2+}$ were used for this measurement to avoid underestimation of break-in current due to fast inflow of $Mg^{2+}$ into the cell. For the same reason extracellular solutions employed in the current study did not contain $Mg^{2+}$ salts to avoid accidental increase in internal $[Mg^{2+}]$ due to diffusion of the bath solution into the pipette. While recording instantaneous current-voltage (*I-V*) relations shortly after break-in, we did not observe contaminating Kv1.3 currents, most probably because the 2.5-s depolarizing holding potential was sufficient to inactivate most of these channels. Electrophysiologically

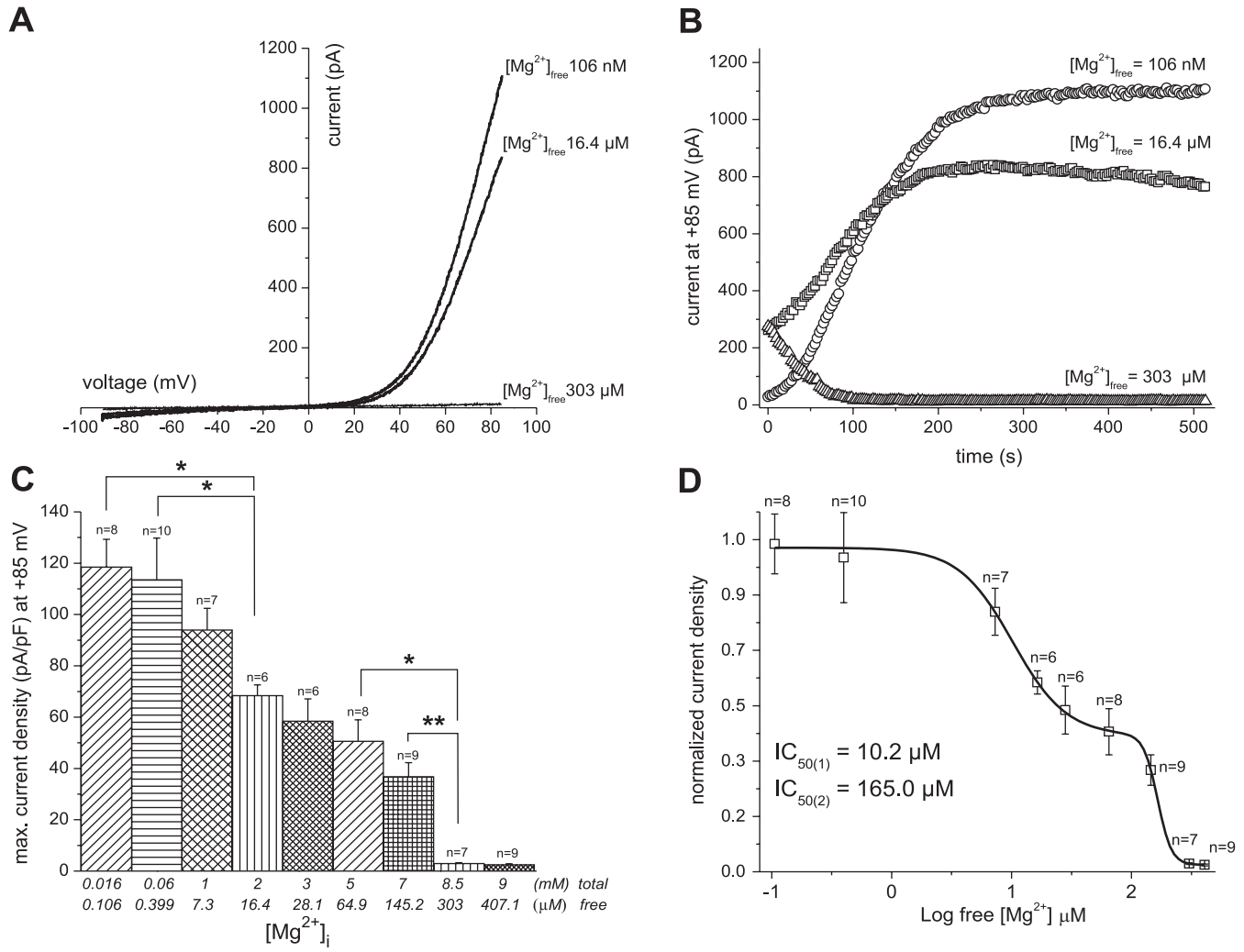


Fig. 2. $Mg^{2+}$ dose-response relation for TRPM7 channels of Jurkat T lymphocytes. *A*: current-voltage (*I-V*) relations for TRPM7 channels from 3 cells containing 106 nM, 16.4 μM, and 303 μM free $Mg^{2+}$. *I-V* relations were taken at the time point when current magnitude reached maximum for each cell. Current amplitudes were obtained from the 120th ramp. *B*: time course of development of TRPM7 current from the same cells as in *panel A*, measured at +85 mV. Note that 303 μM $Mg^{2+}$ inhibits preactivated TRPM7 current (triangles) whereas 16.4 μM $Mg^{2+}$ does not. *C*: maximum current density measurements from Jurkat T cells perfused with various $Mg^{2+}$-containing solutions indicated on the *x*-axis. Number of cells for each concentration is shown at *top* of bar. Here and in Figs. 3 and 4, significant differences between pairs of mean currents are indicated by * (Tukey method) and ** (contrast analysis). Not all pairwise comparisons are shown in the graph. *D*: dose-response relation for internal $Mg^2$ on a logarithmic scale. The fit is a biphasic dose-response curve provided by Origin software fitting subroutine (adjusted *R*-square = 0.99), giving $IC_{50}$ values of 10.2 μM (SE = 0.55) and 165.0 μM (SE = 3.38) with Hill coefficients of 1.92 and 7.62, respectively. Here and in the other figures, data points represent means and SE.

Kv1.3 currents can be distinguished from TRPM7 by its characteristic sigmoidal *I-V* relation (5).

Channel rundown was defined as a reduction in current amplitude during a prolonged recording (21, 22). To compare the extent of rundown we confined our analysis to recordings that lasted at least 12 min, which was sufficient time to induce rundown in most Jurkat T cells.

Salts used were from Acros Organics and Sigma-Aldrich. 1.0 M $MgCl_2$ standard solution was from Fluka. Primers were from Integrated DNA Technologies. Data are presented as means ± SE. All experiments were performed at room temperature.

*Statistical analysis.* One-way ANOVA ($P < 0.0001$) was used for multiple comparisons with the Tukey post hoc method of pairwise comparisons in Figs. 2–4. For some adjacent concentration pairs, effects on current densities were compared with post hoc tests using contrast statements with Bonferroni correction. Differences were considered significant when $P < 0.05$.

## RESULTS AND DISCUSSION

*Internal $Mg^{2+}$ sensitivity.* The goal of the present investigation was to construct a detailed concentration-response curve for intracellular $Mg^{2+}$ $(Mg^{2+})_i$ and $pH_i$ dependence of TRPM7 channels. We and others have shown that millimolar $[Mg^{2+}]$ is sufficient to inhibit endogenous TRPM7 channels of Jurkat T, RBL, and other cell types where they are expressed (12, 17, 21, 40, 43). A similar dependence was observed for the recombinant channels overexpressed heterologously (38). We attempted to get a more detailed description of the $Mg^{2+}$ sensitivity of the native human TRPM7 channels. We used maximal current density as a direct measure of channel activity. Whole cell maximal current amplitude/current density is a compound measurement that depends on several factors, such as the speed of buffer diffusion, the total number of functional channels in

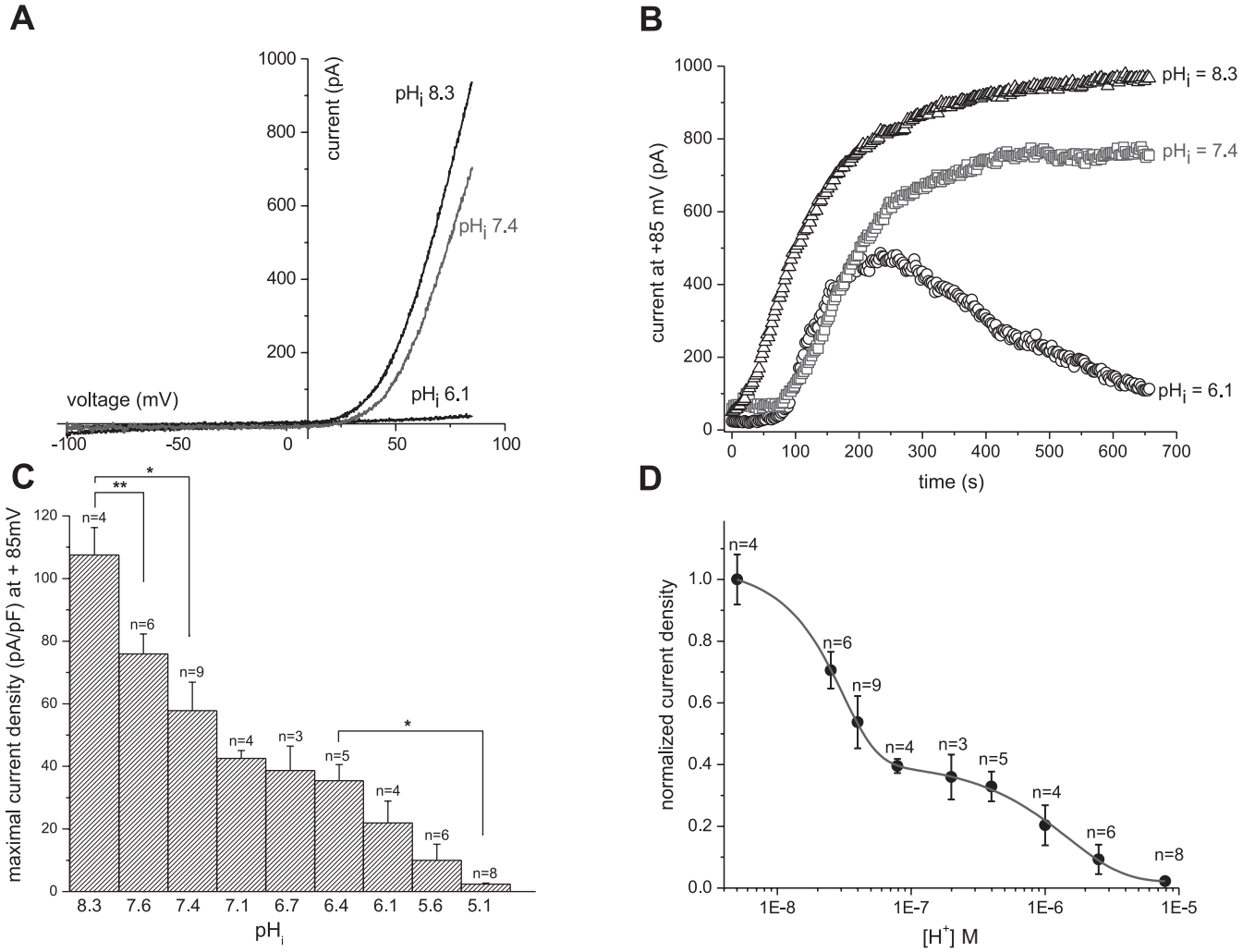


Fig. 3. pH dose-response relation for TRPM7 channels in HEK293 cells obtained with EGTA-containing solutions. *A*: maximally activated *I-V* relations from 3 different HEK293 cells perfused internally with pH 8.3, 7.4, and 6.1, and 12 mM EGTA. *B*: time courses of TRPM7 current development in the same cells as in panel *A*, measured at +85 mV. Note the development and rundown of the proton-activated current at intracellular pH (pH$_i$) of 6.1. *C*: bar graphs showing maximal TRPM7 current densities for internal solutions containing 12 mM EGTA at pH values of 8.3 to 5.1. Not all pairwise comparisons are shown in the graph. *D*: dose-response relation resulting from data in panel *B* normalized to maximum current amplitude is fitted with biphasic dose-response curve (adjusted *R*-square = 0.99), giving IC$_{50}$ values of pH 7.57 (SE = 0.02) and 5.93 (SE = 0.04). Significant differences between pairs of mean currents are indicated by * (Tukey method) and ** (contrast analysis).

the cell membrane, and the extent of rundown during prolonged dialysis (22). Its main advantage is that this is the most physiologically relevant measure of channel activity and the most common one and it does not depend on the cell size. Therefore findings from this type of measurement will be of wider interest since most studies of TRPM7 deal with whole cell recordings of this channel current. This experimental parameter was measured at various internal $Mg^{2+}$ concentrations and a dose-response curve generated. Figure 2*A* shows instantaneous *I-V* plots generated from three Jurkat T cells perfused with the indicated free [$Mg^{2+}$]. The *I-V* relation of native Jurkat T cell TRPM7 channels was steeply outwardly rectifying in presence and absence of internal $Mg^{2+}$. The shape of the *I-V* relation was not altered by $Mg^{2+}{}_i$, suggesting that voltage-dependent pore block is not involved (21). At 106 nM and 16.4 μM [$Mg^{2+}$] TRPM7 current magnitude increased over the time course of several minutes, reaching maximum amplitude after ~5 min of cell dialysis (Fig. 2*B*, circles and squares). Inclusion of 303 μM $Mg^{2+}$ resulted in gradual disappearance of the preactivated current (the current available at $t = 0$ s; see MATERIALS AND METHODS) (Fig. 2*B*, triangles). Repeating these measurements for free $Mg^{2+}$ concentrations of 400 nM to 407 μM and normalizing to cell capacitance, we generated a bar graph plot of maximum current density dependence on [$Mg^{2+}$]$_i$ (Fig. 2*C*). A concentration-response relationship was constructed from data shown in Fig. 2C and is depicted in Fig. 2D. Surprisingly, we found that the data could best be fitted with biphasic dose-response function. We propose that it reflects the existence of two $Mg^{2+}$ inhibitor sites: a high-affinity (~10 μM) and a low-affinity (~165 μM) one. Nanomolar concentrations do not noticeably reduce maximum current density, whereas 300–400 μM $Mg^{2+}$ is sufficient for complete inhibition. Significant total current reduction becomes apparent with low micromolar $Mg^{2+}$ concentrations.

In addition to the apparent maximum current density, channel rundown also appears to be influenced by micromolar

internal [$Mg^{2+}$]. In 17 of a total of 17 cells tested, no rundown was observed when the internal solutions contained 106–400 nM free $Mg^{2+}$. However, with internal solutions containing 7.3–28.1 μM free $Mg^{2+}$, we observed rundown in 8 of 8 cells. This is consistent with our previous findings in RBL cells, where rundown was prevented by EDTA-based solutions containing nanomolar free $Mg^{2+}$ (Ref. 22; Fig. 5).

*Internal pH sensitivity.* Using extracellular weak acids and direct application of low-pH solutions, we previously demonstrated that TRPM7 channels can be inhibited by acidic pH in whole cell and cell-free patches. Conversely, intracellular alkalinization was found to be sufficient to activate these channels even without $Mg^{2+}$ depletion (22). Proton inhibition shares certain features with $Mg^{2+}$ effects, such as voltage

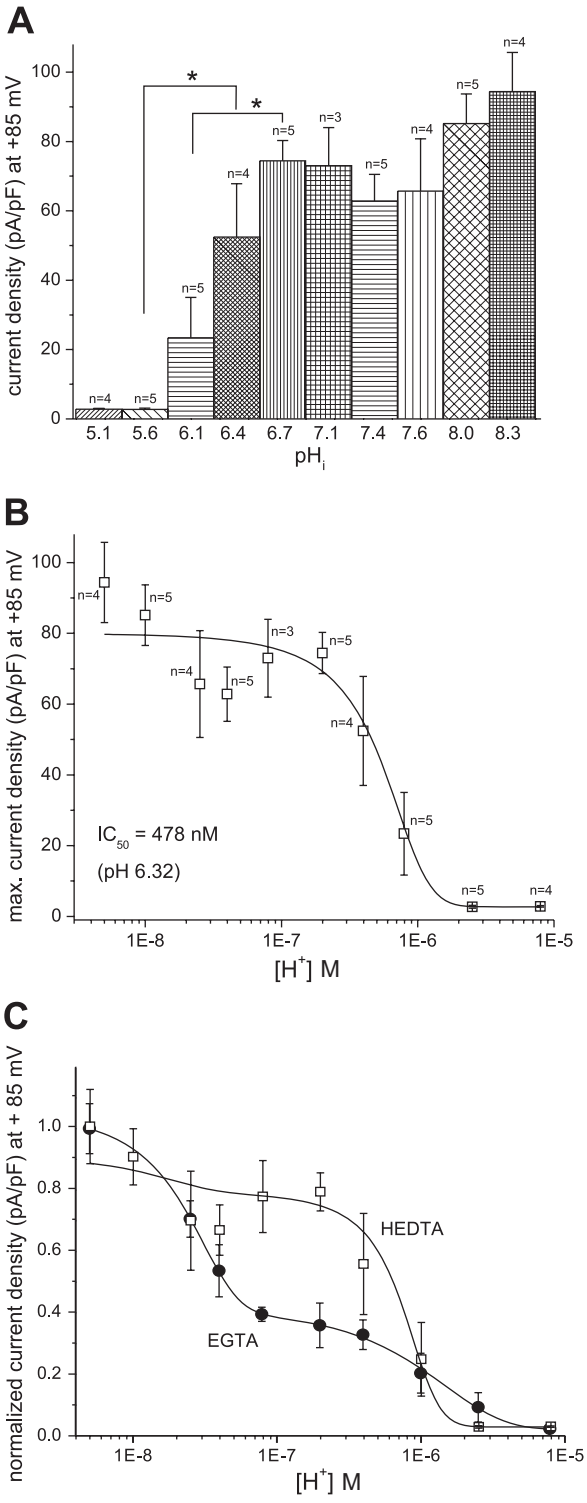


Fig. 4. Dose-response relation for pH dependence of TRPM7 channels in HEK293 cells obtained with *N*-(2-hydroxyethyl)ethylenediaminetriacetate (HEDTA)-containing solutions. *A*: mean TRPM7 current densities at various $pH_i$ values for HEDTA-containing internal solution (measured at ramp 250). Not all pairwise comparisons are shown. *B*: concentration-response relation derived from data in panel *A* plotted against proton concentration on *x*-axis and fitted with standard monophasic dose-response curve (adjusted *R*-square = 0.97) giving $H^+$ concentration ([$H^+$]) $IC_{50}$ value of 478 nM (SE = 89.8 nM) (corresponds to pH 6.32). *C*: superimposed concentration-response relations from Fig. 3*D* (black circles) and 3*B* (open squares) fitted with biphasic dose-response curves. Note that the first deflection seen at pH values of 8.3–7.4 is abolished and the decline at pH values of 6.7 and lower is accelerated for HEDTA-containing solutions. Significant differences between pairs of mean currents are indicated by * (Tukey method).

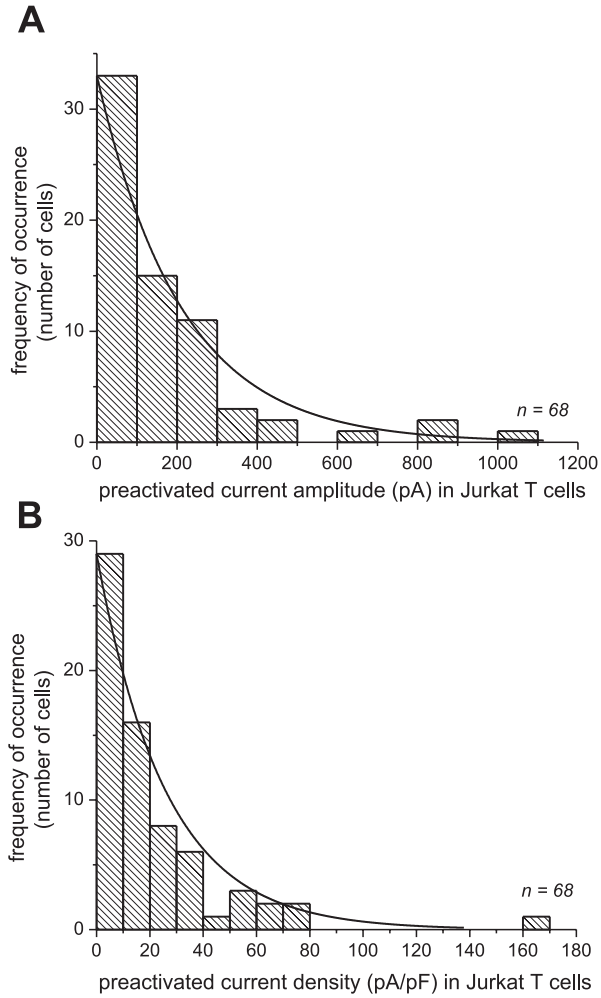


Fig. 5. Amplitude histograms of preactivated TRPM7 currents and current densities in Jurkat T lymphocytes. Current amplitudes were measured at +85 mV for internal solutions containing 106, 266, and 399.5 nM free $Mg^{2+}$. In panel *B*, the same measurements were normalized to cell capacitance and plotted as in panel *A*. The *y*-axis is the number of cells expressing current amplitudes/densities indicated on *x*-axis. No leak subtraction was performed (*A, B*). Histograms in panels *A* and *B* were fitted with monoexponential decay functions.

independence and its slow time course. Moreover, TRPM7 channel rundown can be reversed without addition of phosphatidylinositol-(4,5)-bisphosphate [$PI(4,5)P_2$], by simply alkalinizing the cytoplasm (22). We set out to construct a detailed concentration-response relation for pH inhibition in HEK293, a cell line used by us and others for heterologous expression studies of TRPM7. HEK293 cells express significant endogenous TRPM7 currents, which are poorly characterized despite the fact that this line is used widely as a background line for studies of TRPM7 and other TRP family member expression.

In experiments analogous to those described in Fig. 2, we varied the intracellular pH and measured the corresponding maximum current amplitudes in HEK293 cells. The intracellular solutions contained 12 mM EGTA and no added $Mg^{2+}$. Figure 3*A* shows TRPM7 *I-V* relations when the internal solutions had pH values of 6.1, 7.4, and 8.3. Like $Mg^{2+}$, internal protons did not modify the shape of the *I-V*, suggesting a mechanism that does not involve the ion conduction pathway. Figure 3*B* shows the time course of development of TRPM7 current in HEK293 for the three cells shown in Fig. 3*A*. The transient current seen with pH 6.1 (circles) reflects the activation and rundown of a proton-activated current endogenous to HEK293 cells. Presence of this conductance complicated our measurements at low pH values, and only recordings where this channel ran down early were included in this study. From experiments like one shown in Fig. 2*B*, we constructed a detailed bar graph of the effect of intracellular pH on maximum current density (Fig. 3*C*). The current densities using standard internal solution were somewhat lower than those found in Jurkat T cells. A concentration-response relation was constructed from data in Fig. 3*C* and is depicted in Fig. 3*D*. As with $Mg^{2+}$, the pH dose-response curve shows biphasic behavior, suggesting that two titratable sites exist that govern pH dependence.

We repeated the experiments described in Fig. 3 generating a bar graph of current densities at various pH values with HEDTA-containing internal solution (Fig. 4*A*) and constructing a concentration-response curve that is montonically decreasing and yields an $IC_{50}$ value of 478 nM [$H^+$], which corresponds to pH 6.32.(Fig. 4*B*). What we find is that when EGTA is replaced with HEDTA, the inflection of the curve near this high-affinity site disappeared and the relation becomes monophasic and also shows a steeper decline (Fig. 4*C*). This suggests that the true pH dependence has only one site, and the high-affinity site is in fact occupied by micromolar $Mg^{2+}$ when EGTA is used. When HEDTA was used instead of EGTA, the free $Mg^{2+}$ concentration presumably dropped to nanomolar levels and the contribution of the high-affinity site disappeared as a consequence. HEDTA, being a stronger chelator of $Mg^{2+}$ than EGTA, leaves the micromolar $Mg^{2+}$ binding site unoccupied. It is likely that at more basic pH values EGTA chelated residual $Mg^{2+}$ in the solution more strongly (50), explaining the first inflection of the biphasic curve (Fig. 3). Therefore, even though both intracellular protons and $Mg^{2+}$ inhibit TRPM7 in a similar, voltage-independent manner, they appear not to be identical in nature. The micromolar (high affinity) $Mg^{2+}$ inhibitor site does not have an equivalent in the pH dose-response curve. In other words, protons do not substitute for $Mg^{2+}$ by binding to this site. It appears that protons are able to substitute only for the low-affinity $Mg^{2+}$ inhibitor site (Fig. 3).

Since micromolar $Mg^{2+}$ is necessary for rundown (22), we hypothesize that inhibition caused by micromolar $Mg^{2+}$ in fact reflects increased TRPM7 channel rundown and consequent reduction in maximal current achievable. If pH (protons) could substitute for the high-affinity $Mg^{2+}$ inhibitor site in the absence of $Mg^{2+}$ (HEDTA), then we would expect to observe channel rundown at pH values of 7.4, 7.1, and 6.7 (Fig. 3, *B* and *C*). Strikingly, no rundown was observed in 25 of 25 cells perfused with HEDTA at pH values ranging from 6.7 to 8.3. In contrast, in 11 of 17 cells we observed rundown when the internal buffer was EGTA, presumably because the contaminating $Mg^{2+}$ reached micromolar levels. We conclude that the high-affinity $Mg^{2+}$ inhibitor site is responsible for channel rundown, and protons effectively cannot interact with this site in place of $Mg^{2+}$.

*Preactivation of TRPM7 current in Jurkat T cells.* For the TRPM7 channels to participate in Jurkat T cell ion fluxes it needs to be active in the intact cell without interventions like cell dialysis with $Mg^{2+}$-free solutions or exposure to hypotonic media (40). We set out to characterize the degree of current preactivation (see MATERIALS AND METHODS) in Jurkat T cells, a commonly used model of signal transduction in the human T lymphocyte (2, 3, 11, 29, 49, 51, 53). Instantaneous *I-V* curves were recorded immediately after break-in (delay of ~3 s), before any significant dilution of cytosolic contents took place. Such measurements are expected to provide information on the state of the channels in an intact cell since both inhibition and activation of TRPM7 channels occur on a significantly slower time scale (22; Figs. 2*B* and 3*B*). The current amplitudes were measured at +85 mV (Fig. 5*A*) and normalized to cell capacitance (Fig. 5*B*). In the absence of leak subtraction, this normalization procedure would reduce the contamination of the recordings with nonspecific, linear leak conductance, which is dependent on cell surface area.

The amplitude histogram of preactivated TRPM7 currents shows that the majority of Jurkat T cells have a small current at break-in yet some have significant outward currents (Fig. 5). Free $Mg^{2+}$ levels in T lymphocytes are estimated to be in the 0.5- to 1-mM range (39, 46); therefore, it is surprising that there are active channels even at $Mg^{2+}$ concentrations sufficient for their full inhibition (Fig. 2). One possible factor explaining this observation might be reduced $Mg^{2+}$ levels in the cytoplasm of a given cell. Recently a form of human T-cell immunodeficiency has been described that is caused by defective $Mg^{2+}$ influx through MAGT1 transporter, resulting in low basal $Mg^{2+}$ levels in T cells (30); therefore such a preactivation mechanism is possible. In our view, a more likely explanation would involve alkalinization of the cytoplasm caused by unknown factors. BCECF dye-based pH measurements in Jurkat T cells show that some batches of cells have unexpectedly high resting pH values, ~8.4 (Kozak, unpublished observations; see also Ref. 24) . This pH value would be sufficient to activate a significant portion of the channels even in the absence of $Mg^{2+}$ depletion (22). Last, another component of tonic inhibition of TRPM7 channels are the cellular polyamines (22), and their depletion would also be expected to favor channel preactivation. In our previous publications we encountered spontaneously preactivated TRPM7 currents in rat PAS (20) and RBL cells (22).

TRP channels are thought to act to depolarize the membrane when open (45, 57). We hypothesize that as with other TRP

channels, preactivation of TRPM7 will tend to depolarize the T cell and bring its membrane potential closer to ~0 mV. This would be expected to reduce the driving force for $Ca^{2+}$ entry and counteract $Ca^{2+}$ elevations caused by store-operated $Ca^{2+}$ entry (i.e., Orai1 channels). Such a role has been reported for TRPM4 channels in T cells (25). Activation of voltage-gated and $Ca^{2+}$-activated $K^+$ channels in T lymphocytes, on the contrary, results in an increased driving force for $Ca^{2+}$ due to membrane hyperpolarization (9, 27, 28). Reduced driving force for $Ca^{2+}$ entry into the lymphocyte reduces the amount of $Ca^{2+}$ accumulation in the cytoplasm and results in diminished activity of $Ca^{2+}$-sensitive transcription factors such as nuclear factor of activated T cells (NF-AT). Reduced NF-AT activation, in turn, would be expected to downregulate the expression of IL-2, a lymphokine necessary for T-cell activation and proliferation (4, 54). Thus $K^+$ channel blockers inhibit mitogen-induced T-cell proliferation and IL-2 production, primarily by depolarizing the membrane (9, 19, 41). Therefore, we hypothesize, that preactivation of a depolarizing TRPM7 conductance in T lymphocytes would inhibit their activation and proliferation and their adaptive immune function. Further studies are needed to address the participation of TRPM7 conductance in setting resting Jurkat T cell membrane potential.

In the present study we have made no attempt to locate the two $Mg^{2+}$ binding sites within the TRPM7 protein. Previously we suggested that $Mg^{2+}$- and proton-induced inhibition reflects the screening (shielding) of negative charges on anionic lipids, such as $PI(4,5)P_2$, that positively regulate TRPM7 activity. Similar to potassium channels (8), TRPM7 channel activity is diminished during prolonged patch-clamp recording and can be recovered when $PI(4,5)P_2$ is applied to the inner side of the membrane in cell-free patches (22, 47). In cardiac myocytes, rundown of whole cell TRPM7-like current is reduced when internal solutions contain micromolar $PI(4,5)P_2$ (31). Whether both $Mg^{2+}$ inhibitor sites that we report here involve screening of phosphoinositides or other anionic lipids remains to be discovered. For the bacterial KcsA potassium channel it has been demonstrated that activation involves both annular (surrounding the protein) and nonannular (within the protein) interactions with anionic phospholipid (26, 33, 52). It is therefore possible that the two $Mg^{2+}$ sites of TRPM7 inhibition reflect differential shielding of annular and nonannular phospholipid interactions. Future, detailed single-channel analysis will elucidate the elementary parameters that are reduced by intracellular $Mg^{2+}$ and acidic pH during TRPM7 channel inhibition.

## ACKNOWLEDGMENTS

We thank O. Bennett for technical assistance, Tom L. Brown for the gift of Jurkat T lymphocytes and Mark M. Rich for reading the manuscript and helpful comments.

## GRANTS

This work was funded by the American Heart Association, National Center and National Institute of Allergy and Infectious Diseases (J. A. Kozak).

## DISCLOSURES

No conflicts of interest, financial or otherwise, are declared by the author(s).

## AUTHOR CONTRIBUTIONS

Author contributions: R.C. performed experiments; R.C. and J.A.K. analyzed data; M.M. and J.A.K. conception and design of research; J.A.K. interpreted results of experiments; J.A.K. prepared figures; J.A.K. drafted manuscript; J.A.K. edited and revised manuscript; J.A.K. approved final version of manuscript.

## REFERENCES

1. **Bates-Withers C, Sah R, Clapham DE.** TRPM7, the $Mg^{2+}$ inhibited channel and kinase. *Adv Exp Med Biol* 704: 173–183, 2011.
2. **Brown TJ, Shuford WW, Wang WC, Nadler SG, Bailey TS, Marquardt H, Mittler RS.** Characterization of a CD43/leukosialin-mediated pathway for inducing apoptosis in human T-lymphoblastoid cells. *J Biol Chem* 271: 27686–27695, 1996.
3. **Brown TL.** Q-VD-OPh, next generation caspase inhibitor. *Adv Exp Med Biol* 559: 293–300, 2004.
4. **Cahalan MD, Chandy KG.** The functional network of ion channels in T lymphocytes. *Immunol Rev* 231: 59–87, 2009.
5. **Cahalan MD, Chandy KG, DeCoursey TE, Gupta S, Lewis RS, Sutro JB.** Ion channels in T lymphocytes. *Adv Exp Med Biol* 213: 85–101, 1987.
6. **Chokshi RH, Matsushita M, Kozak JA.** Detailed examination of TRPM7 channel $Mg^{2+}$ dependence (Abstract). In: *Proc Ohio Physiol Soc Annu Mtg 26th*. Cincinnati, OH: Univ. of Cincinnati, 2011.
7. **Clapham DE.** TRP channels as cellular sensors. *Nature* 426: 517–524, 2003.
8. **Fan Z, Makielski JC.** Anionic phospholipids activate ATP-sensitive potassium channels. *J Biol Chem* 272: 5388–5395, 1997.
9. **Fanger CM, Rauer H, Neben AL, Miller MJ, Rauer H, Wulff H, Rosa JC, Ganellin CR, Chandy KG, Cahalan MD.** Calcium-activated potassium channels sustain calcium signaling in T lymphocytes. Selective blockers and manipulated channel expression levels. *J Biol Chem* 276: 12249–12256, 2001.
10. **Gallin EK.** Ion channels in leukocytes. *Physiol Rev* 71: 775–811, 1991.
11. **Guse AH, da Silva CP, Emmrich F, Ashamu GA, Potter BV, Mayr GW.** Characterization of cyclic adenosine diphosphate-ribose-induced $Ca^{2+}$ release in T lymphocyte cell lines. *J Immunol* 155: 3353–3359, 1995.
12. **Gwanyanya A, Amuzescu B, Zakharov SI, Macianskiene R, Sipido KR, Bolotina VM, Vereecke J, Mubagwa K.** Magnesium-inhibited, TRPM6/7-like channel in cardiac myocytes: permeation of divalent cations and pH-mediated regulation. *J Physiol* 559: 761–776, 2004.
13. **Hardie RC.** A brief history of trp: commentary and personal perspective. *Pflügers Arch* 461: 493–498, 2011.
14. **Hardie RC, Minke B.** The trp gene is essential for a light-activated $Ca^{2+}$ channel in *Drosophila* photoreceptors. *Neuron* 8: 643–651, 1992.
15. **Hermosura MC, Monteilh-Zoller MK, Scharenberg AM, Penner R, Fleig A.** Dissociation of the store-operated calcium current I(CRAC) and the Mg-nucleotide-regulated metal ion current MagNuM. *J Physiol* 539: 445–458, 2002.
16. **Inoue K, Branigan D, Xiong ZG.** Zinc-induced neurotoxicity mediated by transient receptor potential melastatin 7 channels. *J Biol Chem* 285: 7430–7439, 2010.
17. **Jiang X, Newell EW, Schlichter LC.** Regulation of a TRPM7-like current in rat brain microglia. *J Biol Chem* 278: 42867–42876, 2003.
18. **Kerschbaum HH, Kozak JA, Cahalan MD.** Polyvalent cations as permeant probes of MIC and TRPM7 pores. *Biophys J* 84: 2293–2305, 2003.
19. **Koo GC, Blake JT, Talento A, Nguyen M, Lin S, Sirotina A, Shah K, Mulvany K, Hora D Jr, Cunningham P, Wunderler DL, McManus OB, Slaughter R, Bugianesi R, Felix J, Garcia M, Williamson J, Kaczorowski G, Sigal NH, Springer MS, Feeney W.** Blockade of the voltage-gated potassium channel Kv1.3 inhibits immune responses in vivo. *J Immunol* 158: 5120–5128, 1997.
20. **Kozak JA, Cahalan MD.** MIC channels are inhibited by internal divalent cations but not ATP. *Biophys J* 84: 922–927, 2003.
21. **Kozak JA, Kerschbaum HH, Cahalan MD.** Distinct properties of CRAC and MIC channels in RBL cells. *J Gen Physiol* 120: 221–235, 2002.
22. **Kozak JA, Matsushita M, Nairn AC, Cahalan MD.** Charge screening by internal pH and polyvalent cations as a mechanism for activation, inhibition, and rundown of TRPM7/MIC channels. *J Gen Physiol* 126: 499–514, 2005.
23. **Kuo CC, Hess P.** Block of the L-type $Ca^{2+}$ channel pore by external and internal $Mg^{2+}$ in rat phaeochromocytoma cells. *J Physiol* 466: 683–706, 1993.
24. **Lang F, Madlung J, Bock J, Lukewille U, Kaltenbach S, Lang KS, Belka C, Wagner CA, Lang HJ, Gulbins E, Lepple-Wienhues A.**

Inhibition of Jurkat-T-lymphocyte $Na^+/H^+$-exchanger by CD95(Fas/Apo-1)-receptor stimulation. *Pflügers Arch* 440: 902–907, 2000.
25. **Launay P, Fleig A, Perraud AL, Scharenberg AM, Penner R, Kinet JP.** TRPM4 is a $Ca^{2+}$-activated nonselective cation channel mediating cell membrane depolarization. *Cell* 109: 397–407, 2002.
26. **Lee AG.** Lipid-protein interactions. *Biochem Soc Trans* 39: 761–766, 2011.
27. **Lee SC, Levy DI, Deutsch C.** Diverse $K^+$ channels in primary human T lymphocytes. *J Gen Physiol* 99: 771–793, 1992.
28. **Lewis RS.** Calcium signaling mechanisms in T lymphocytes. *Annu Rev Immunol* 19: 497–521, 2001.
29. **Lewis RS, Cahalan MD.** Mitogen-induced oscillations of cytosolic $Ca^{2+}$ and transmembrane $Ca^{2+}$ current in human leukemic T cells. *Cell Regul* 1: 99–112, 1989.
30. **Li FY, Chaigne-Delalande B, Kanellopoulou C, Davis JC, Matthews HF, Douek DC, Cohen JI, Uzel G, Su HC, Lenardo MJ.** Second messenger role for $Mg^{2+}$ revealed by human T-cell immunodeficiency. *Nature* 475: 471–476, 2011.
31. **Macianskiene R, Gwanyanya A, Vereecke J, Mubagwa K.** Inhibition of the magnesium-sensitive TRPM7-like channel in cardiac myocytes by nonhydrolysable GTP analogs: involvement of phosphoinositide metabolism. *Cell Physiol Biochem* 22: 109–118, 2008.
32. **Manning G, Whyte DB, Martinez R, Hunter T, Sudarsanam S.** The protein kinase complement of the human genome. *Science* 298: 1912–1934, 2002.
33. **Marius P, Zagnoni M, Sandison ME, East JM, Morgan H, Lee AG.** Binding of anionic lipids to at least three nonannular sites on the potassium channel KcsA is required for channel opening. *Biophys J* 94: 1689–1698, 2008.
34. **Matsushita M, Kozak JA, Shimizu Y, McLachlin DT, Yamaguchi H, Wei FY, Tomizawa K, Matsui H, Chait BT, Cahalan MD, Nairn AC.** Channel function is dissociated from the intrinsic kinase activity and autophosphorylation of TRPM7/ChaK1. *J Biol Chem* 280: 20793–20803, 2005.
35. **Monteilh-Zoller MK, Hermosura MC, Nadler MJ, Scharenberg AM, Penner R, Fleig A.** TRPM7 provides an ion channel mechanism for cellular entry of trace metal ions. *J Gen Physiol* 121: 49–60, 2003.
36. **Montell C.** $Mg^{2+}$ homeostasis: the Mg(2+)nificent TRPM chanzymes. *Curr Biol* 13: R799–R801, 2003.
37. **Montell C, Birnbaumer L, Flockerzi V.** The TRP channels, a remarkably functional family. *Cell* 108: 595–598, 2002.
38. **Nadler MJ, Hermosura MC, Inabe K, Perraud AL, Zhu Q, Stokes AJ, Kurosaki T, Kinet JP, Penner R, Scharenberg AM, Fleig A.** LTRPC7 is a Mg ATP-regulated divalent cation channel required for cell viability. *Nature* 411: 590–595, 2001.
39. **Ng LL, Davies JE, Garrido MC.** Intracellular free magnesium in human lymphocytes and the response to lectins. *Clin Sci (Lond)* 80: 539–547, 1991.
40. **Numata T, Shimizu T, Okada Y.** TRPM7 is a stretch- and swelling-activated cation channel involved in volume regulation in human epithelial cells. *Am J Physiol Cell Physiol* 292: C460–C467, 2007.
41. **Panyi G, Varga Z, Gaspar R.** Ion channels and lymphocyte activation. *Immunol Lett* 92: 55–66, 2004.
42. **Phillips AM, Bull A, Kelly LE.** Identification of a *Drosophila* gene encoding a calmodulin-binding protein with homology to the trp phototransduction gene. *Neuron* 8: 631–642, 1992.
43. **Prakriya M, Lewis RS.** Separation and characterization of currents through store-operated CRAC channels and $Mg^{2+}$-inhibited cation (MIC) channels. *J Gen Physiol* 119: 487–507, 2002.
44. **Quamme GA.** Molecular identification of ancient and modern mammalian magnesium transporters. *Am J Physiol Cell Physiol* 298: C407–C429, 2010.
45. **Ramsey IS, Delling M, Clapham DE.** An introduction to TRP channels. *Annu Rev Physiol* 68: 619–647, 2006.
46. **Rink TJ, Tsien RY, Pozzan T.** Cytoplasmic pH and free $Mg^{2+}$ in lymphocytes. *J Cell Biol* 95: 189–196, 1982.
47. **Runnels LW, Yue L, Clapham DE.** The TRPM7 channel is inactivated by PIP(2) hydrolysis. *Nat Cell Biol* 4: 329–336, 2002.
48. **Schmitz C, Perraud AL, Johnson CO, Inabe K, Smith MK, Penner R, Kurosaki T, Fleig A, Scharenberg AM.** Regulation of vertebrate cellular $Mg^{2+}$ homeostasis by TRPM7. *Cell* 114: 191–200, 2003.
49. **Schneider U, Schwenk HU, Bornkamm G.** Characterization of EBV-genome negative "null" and "T" cell lines derived from children with acute lymphoblastic leukemia and leukemic transformed non-Hodgkin lymphoma. *Int J Cancer* 19: 621–626, 1977.
50. **Schoenmakers TJ, Visser GJ, Flik G, Theuvenet AP.** CHELATOR: an improved method for computing metal ion concentrations in physiological solutions. *Biotechniques* 12: 870–874, 876–879, 1992.
51. **Timmerman LA, Clipstone NA, Ho SN, Northrop JP, Crabtree GR.** Rapid shuttling of NF-AT in discrimination of $Ca^{2+}$ signals and immunosuppression. *Nature* 383: 837–840, 1996.
52. **Valiyaveetil FI, Zhou Y, MacKinnon R.** Lipids in the structure, folding, and function of the KcsA $K^+$ channel. *Biochemistry* 41: 10771–10777, 2002.
53. **Weiss A, Imboden J, Shoback D, Stobo J.** Role of T3 surface molecules in human T-cell activation: T3-dependent activation results in an increase in cytoplasmic free calcium. *Proc Natl Acad Sci USA* 81: 4169–4173, 1984.
54. **Weiss A, Samelson LE.** T lymphocyte activation. In: *Fundamental Immunology* (5th ed.), edited by Paul WE. Philadelphia, PA: Lippincott Williams and Wilkins, 2003, p. 321–364.
55. **Wolf FI.** TRPM7: channeling the future of cellular magnesium homeostasis? *Sci STKE* 2004: pe23, 2004.
56. **Yamaguchi H, Matsushita M, Nairn AC, Kuriyan J.** Crystal structure of the atypical protein kinase domain of a TRP channel with phosphotransferase activity. *Mol Cell* 7: 1047–1057, 2001.
57. **Yu PC, Du JL.** Transient receptor potential canonical channels in angiogenesis and axon guidance. *Cell Mol Life Sci*, 2011.
58. **Yu SP, Kerchner GA.** Endogenous voltage-gated potassium channels in human embryonic kidney (HEK293) cells. *J Neurosci Res* 52: 612–617, 1998.